Journal Pre-proof

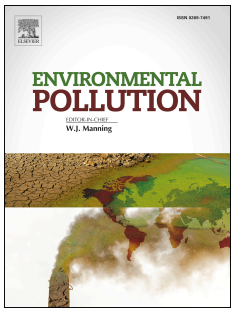

Size-dependent effects of polystyrene micro- and nanoplastics on the quality of rice grains and the metabolism mechanism

Xiangrui Miao, Wei Wang, Lizhong Zhu

PII: S0269-7491(25)00836-X

DOI: https://doi.org/10.1016/j.envpol.2025.126463

Reference: ENPO 126463

To appear in: *Environmental Pollution*

Received Date: 26 February 2025

Revised Date: 24 April 2025

Accepted Date: 14 May 2025

Please cite this article as: Miao, X., Wang, W., Zhu, L., Size-dependent effects of polystyrene micro- and nanoplastics on the quality of rice grains and the metabolism mechanism, *Environmental Pollution*, https://doi.org/10.1016/j.envpol.2025.126463.

Size-dependent effects of polystyrene micro- and nanoplastics on the quality of rice grains and the metabolism mechanism

Xiangrui Miao[a, b], Wei Wang[a, b,*], Lizhong Zhu[a, b]

[a] Key Laboratory of Soil Pollution Control and Safety, Hangzhou, Zhejiang, 310058, China

[b] College of Environmental and Resource Sciences, Zhejiang University, Hangzhou, Zhejiang, 310058, China

*Corresponding author: Wei Wang

Phone: +86-0571-88982176

E-mail: wwl@zju.edu.cn

ORCID ID: 0000-0001-7066-6076

Abstract

Micro- and nanoplastics (MNPs) exhibited size-dependent impacts on crop physiological processes and metabolic functions, ultimately threatening crop quality. The size-specific response patterns warrant close attention to enable a more accurate assessment of their environmental and human health risks. In this study, both soil (10 mg/kg and 100 mg/kg) and hydroponic (1 μg/L and 10 μg/L) exposure systems were employed to investigate the effects of six spherical polystyrene (PS) MNPs particle diameters (80, 100, 200, 500, 800, and 1000 nm) on the grain quality of rice (*Oryza sativa* L.), and to further elucidate the underlying metabolic mechanisms. The results indicated that PS MNPs were absorbed through rice roots and transported upward, with concentrations in rice leaves ranging from 297 to 701 μg/g. When exposure to PS MNPs with diameters ≤ 100 nm (PS≤100 nm), the reactive oxygen species (ROS) levels in the plants increased by 25%, and glutenin content in the grain decreased by up to 29%. Metabolomic analysis revealed that glycolysis/gluconeogenesis and pentose and glucuronate interconversion in rice leaves were closely associated with the particle diameters of PS MNPs. Compared to larger particles, exposure to PS≤100 nm downregulated carbohydrate metabolism and decreased the accumulation of sugars (starch, soluble sugars), thereby weakening the plant's defense response. This study demonstrated that PS≤100 nm triggered weaker defense response in rice, leading to greater biotoxicity, thereby deserving particular attention for governing the MNPs risk and crop safety assessment.

Keywords: Microplastics, Polystyrene, Rice, Particle size, metabolism, quality

1. Introduction

Micro- and nano plastics (MNPs) pollution poses critical environmental and health risks, calling for urgent global action. The extensive production and usage of plastics have resulted in the release of persistent, invisible, yet pervasive MNPs into the environment (Thompson. et al., 2004). Soil, particularly agricultural soil, functions as a major terrestrial sink for MNPs and serves as an important transmission node for MNPs-related risks (Rillig et al., 2024). MNPs entered agricultural ecosystems via sludge application (Weithmann et al., 2018), wastewater irrigation (Hasan & Tarannum, 2025), and plastic mulching (Qi et al., 2020). Recent surveys have shown that the abundance of MNPs in agricultural soils, particularly paddy soils, ranges from 10.3±2.2 to 3805±511 items/kg (Table S1). Most of these particles are smaller than 1 mm, with fibers and microspheres predominating. The presence of MNPs in agricultural soils may detrimentally interfere with the physiochemical functions of crops, impairing their growth, modifying the carbohydrate and protein levels in crop grains, and consequently affecting quality of edible parts (Hasan & Tarannum, 2025; Jin et al., 2022). Therefore, it was necessary to characterize the impact of MNPs on crop growth, development and crop quality, offering important scientific evidence for accurately regulating the risk of MNPs in agricultural soils.

MNPs disturbed crop quality through the entire life cycle of absorption, distribution and metabolism (Chen et al., 2022; Jamil et al., 2025; Shi et al., 2024). They entered crops via roots cracks (L. Li et al., 2020), were transported upward along the vascular cylinder under transpiration pull (R. Li et al., 2020; Liu et al., 2022), and

eventually reaching edible parts (Jiang et al., 2022). MNPs were capable of generating reactive oxygen species (ROS), triggering antioxidant defense response (e.g., antioxidant enzymes such as superoxide dismutase and peroxidase) (Ma et al., 2022; Zhang et al., 2021), and breaking important biomolecules such as carbohydrates, proteins or DNA (Y. Zhang et al., 2023; Zhou et al., 2021; Zhu et al., 2023). Particularly, sugars, including monosaccharides and oligosaccharides (i.e., soluble sugars), and polysaccharides (e.g., starch) are necessary energy materials for crop growth and development, and also vital substance in stress responses (Keunen et al., 2013). Exposure to MNPs detrimentally consumed soluble sugars to adapt oxidative stress. In response, starch was degraded to supplement soluble sugars and reshape carbohydrate metabolism network, thereby improving plant resilience (Asad et al., 2024; Wu et al., 2022). Therefore, MNPs induce oxidative damage in crops, alter the levels of key biomacromolecules such as carbohydrates and proteins, and disturb the overall balance of the metabolic network, thereby exerting adverse effects on crop physiology and metabolism.

Particle diameters impacted the absorption of MNPs into crops, thus may be exhibited as a determinant of the influence on crop growth, metabolism and grain quality (Shi et al., 2024; Yao et al., 2024). Crops tended to absorb nanoscale plastics (diameter < 100 nm) more efficiently than microscale plastics (diameter > 1 μm), leading to their accumulation within plant tissues (Li et al., 2019; Zhu et al., 2022). Studies indicated that smaller MNPs (e.g., particle diameters of 50 nm and 100 nm) accumulating in plant tissues can obstruct intercellular connections and cell wall pores,

disrupt nutrient transport, and cause greater oxidative damage and metabolic disturbance, ultimately may impair crop quality (Jiang et al., 2019; Zhu et al., 2023). In contrast, microscale plastics tend to enhance photosynthesis in crops, while the plants upregulate antioxidant substances (e.g., soluble sugars, soluble proteins and ascorbic acid) to alleviate the biotoxicity of MNPs (He et al., 2024; Z. Li et al., 2020; C. Zhang et al., 2023). Alterations in crop physiological responses and metabolic homeostasis ultimately result in changes in crop quality. Moreover, MNPs particle diameters can differentially affect crop quality by modulating plant physiological traits, metabolic profiles, and enzyme activities. Thus, we hypothesize that MNPs with specific particle diameter can enter crops, differentially modulate oxidative stress responses, carbohydrates and related proteins synthesis, and the global metabolic network, ultimately exerting distinct effects on crop quality.

Polystyrene (PS), a synthetic polymer made from monomers of the aromatic hydrocarbon styrene, has been one of the most prevalent and hazardous types of microplastics (Kik et al., 2020). Rice, as a staple crop for more than half of the global population, contributes a significant portion of dietary calories worldwide (Paliwal et al., 2018). Therefore, studying the exposure of rice to PS particles of different diameters is of significant interest. This study aimed to characterize the impact of PS particles of varied particle diameters on the quality of rice grains and reveal the underlying biochemical mechanism, using the combination of soil and hydroponic cultivation, electron microscopy characterization, physiochemical responses and omics analysis. The specific objectives included: (1) to evaluate the impact of PS of different diameters

on rice grain quality; (2) to observe the absorption and accumulation of PS of different diameters in rice; (3) to compare the physicochemical responses of rice to PS of varied diameters; and (4) to elucidate the metabolic mechanisms through which PS different diameters affect rice. These findings will provide valuable insights into understanding the behavior of MNPs in plants, evaluating their potential risks to crop yield and quality, and determining the precise threshold for scientific supervision of MNPs risks in agricultural soil.

2. Materials and methods

2.1 MP characterization

Monodisperse PS microspheres with six diameters (80, 100, 200, 500, 800, and 1000 nm), representative of MNPs, were fluorescently labeled with Nile Blue chloride and purchased from Tianjin Big Goose Scientific Co., Ltd. (Tianjin, China). The morphology of the plastic microspheres was characterized using transmission electron microscopy (TEM) (JEOL, JEM – 1400 Flash, Japan), with detailed procedures provided in Text S1 of the Supporting Information. Fluorescence microscope (Olympus, U-RFL-T, Japan) was used to detect the light emitted by plastic microspheres under excitation. The particle diameters distribution and surface charge of the PS MNPs were determined using a zeta potential analyzer (Malvern, Zetasizer Nano ZS, United Kingdom). The chemical composition and functional groups of plastic microspheres were examined using Raman spectroscopy (WiTec, Alpha300R, Germany), with further details provided in Text S2.

2.2 Seed cultivation

Rice seeds (*Oryza sativa* L., Lianjing-6188) were purchased from the Lianyungang Academy of Agricultural Science (Jiangsu, China). The seeds were first rinsed using ultrapure water, and then soaked in ultrapure water for 5 min. After that, the seeds were sterilized by soaking in a 3% H_2O_2 solution for 30 min, followed by a 48-hour incubation in ultrapure water under dark conditions. The seeds were then hydroponically cultivated in 11 liters of Hoagland's nutrient solution (pH 5.5−6.0) in a greenhouse (25 ± 0.5 ℃, 70 ± 5% humidity, 7000 lx, and 14-hour light/10-hour dark cycle). The components of Hoagland nutrient solution were summarized in Table S2.

2.3 Soil cultivation of rice

To investigate the effects of different PS diameters on rice grain quality, a soil cultivation experiment was conducted. Soil was collected from Huai'an in Jiangsu Province (Latitude: 32.2450°N, Longitude: 118.5415°E), with a pH of 7.2 and an electrical conductivity of 3944 μS/cm (Text S3). The soil was initially screened by hand, dried in the sun and sieved through a 2 mm sieve prior to use. PS particles of each diameters were uniformly incorporated into the soil using a stepwise dilution method as previously described (Chen et al., 2019), to obtain three concentration levels: 0 mg/kg (control group), 10 mg/kg, and 100 mg/kg. After a 14-day nursery period, rice seedlings with a height of 20−24 cm were selected and transplanted into buckets (Height of 240 mm, top diameter of 215 mm, bottom diameter of 185 mm, 8 plants per pot, 3 pots per treatment) which contained 5 kg of contaminated soil. Rice was irrigated every 2–3 days as needed to maintain continuous flooding. The soil cultivation experiment was conducted in a greenhouse (14-h photoperiod, 25/20 ℃ day/night

147 temperature, 70% relative humidity). Rice grains were harvested after a cultivation
148 period of 6 months.

149 **2.4 Grain Quality Analysis**

150 After 180 days of soil cultivation, mature rice grains were harvested and dehulled
151 using a rice huller. The dehulled grains were freeze-dried in a freeze dryer (Scientz,
152 Scientz-10 N/A, China) for 48 hours, ground into powder, and sieved through a 0.15-
153 mm mesh sieve for further analysis.

154 Protein, including albumin, globulin, prolamin, and glutenin, were sequentially
155 extracted based on the solubility differences, and were quantified using the
156 bicinchoninic acid (BCA) assay (Beyotime Biotech Inc, Shanghai, China). The method
157 for extracting protein was described in Text S4. Grain starch and total sugars contents
158 were measured using the Solarbio assay kit (Solarbio, Beijing, China).

159 **2.5 Hydroponic cultivation of rice**

160 A hydroponic experiment was conducted to explore the potential mechanisms
161 underlying rice quality changes induced by PS of different particle diameters. After a
162 7-day cultivation period, a total of 24 plants of 15−16 cm length were transferred to
163 brown glass vials that contained 480 mL of Hoagland nutrient solution (pH 5.5) for
164 8−10 days in a greenhouse (25 ± 0.5℃, 70 ± 5% humidity, 7000 lx, and 14 h light/10
165 h dark). Three exposure concentrations of PS, 0 μg/mL (control group),1 μg/mL and 10
166 μg/mL were selected. The rim of the vials were sealed with sponge stoppers to prevent
167 exogenous interference. After 14 days of cultivation, rice seeding leaves and roots were
168 harvested separately for subsequent analyses.

2.6 Uptake and accumulation of PS MNPs in rice roots and leaves

After 14 days of hydroponic cultivation, fresh roots of control group and 1 μg/mL of PS MNPs exposure were collected. The roots were manually sliced into ultra-thin sections using a blade and placed on the surface water. A coverslip was placed over the sections to prepare manual slices. Cross-sections were observed using a laser scanning confocal microscope (Zeiss, LSM 880, Germany).

After 14 days of hydroponic cultivation, fresh leaves of control group, 1 and 10 μg/mL of PS MNPs exposure were collected, stored at -80 °C for 24 hours, and then lyophilized using a freeze dryer (Scientz, Scientz-10 N/A) for 48 hours. The dried rice leaves and roots were ground into powder. The pretreatment method and quantification method for PS MNPs in rice samples followed the approach described by Li et al. (C. Li et al., 2021). A Pyrolysisgas-chromatography/mass spectrometry (Py-GC/MS) system consisting of a microfurnace pyrolyzer (Frontier Laboratories, EGA/Py 3030D, Japan), a GC instrument (ThermoFisher, Trace 1300, USA), and a mass spectrometer (ThermoFisher, ISQ 7000, Singapore) was applied for the analysis of PS MNPs in rice leaves. Quality assurance and quality control (QA/QC) procedures were conducted prior to each analytical batch for mass calibration. Instrumental blanks were analyzed for every six samples. To minimize potential contamination, a piece of quartz wool was placed at the opening of the pyrolysis cup after sample preparation. Experimental details of the Py-GC/MS analysis are provided in Text S5.

2.7 Physiological and Biochemical Analysis

After hydroponic cultivation for 14 days, fresh rice leaves and roots were ground

into powder in liquid nitrogen. Superoxide dismutase (SOD) and peroxidase (POD) activities were determined using the methods reported in previous studies (Charles & Irwin, 1971; Q & Z, 1999). Malondialdehyde (MDA) was determined using the thiobarbituric acid reactive substances (TBARS) method. ROS levels were measured using Meimian assay kits (Jiangsu Meimian industrial CO., Ltd, Jiangsu, China). Soluble sugars content were determined using Solarbio assay kits (Solarbio, Beijing, China).

After 14 days of hydroponic cultivation, fresh rice leaves and roots were harvested, and dried rice samples were prepared using the same method. Proteins were extracted and determined following the method described in Section 2.4.

2.8 Extraction and analysis of metabolites

After 14 days of hydroponic cultivation, 10 mg of ground rice powder from the control group and 1 μg/mL of PS exposure were collected for metabolic analysis, and the metabolite extraction method is provided in Text S6. Metabolites were immediately determined using an ultra-performance liquid chromatography (UPLC) system coupled with an UPLC-QTRAP 5500+ system (SCIEX, Framingham, USA). Analysis was performed using both positive and negative ion scanning modes. Experimental details and instrument parameters for the UPLC analysis are provided in Text S7 and Table S3, respectively. Statistical analysis of metabolomics data was performed using the online MetaboAnalyst 6.0 (http://www.metaboanalyst.ca/).

2.9 QA/QC and Statistical analysis

To minimize contamination, dust-proof clothing and latex gloves were worn

throughout the experiment. Plastic materials were avoided, and metal, glass, or quartz wool were used as substitutes. Each treatment group had at least three biological replicates.

The data were analyzed and visualized using R software, and results are presented as means ± standard deviation. One-way analysis of variance (ANOVA) was used to compare the statistical differences between groups, and Student *t-test* was used to compare the control and treatment groups. A *P*-value less than 0.05 was considered to indicate a statistically significant difference ($P < 0.05$, *; $P < 0.01$, **). To further evaluate the effect size between the treatment and control groups, Cohen's *d* was calculated using Python.

3. Results and discussion

3.1 Characterization of PS MNPs

According to TEM analysis, PS MNPs exhibited a structurally uniform, smooth, spherical morphology with good dispersibility (Fig. 1a−b, Fig. S1). Under the fluorescence microscope, plastic microspheres emitted red fluorescence with a maximum excitation wavelength of 620 nm and a maximum emission wavelength of 680 (Fig. 1c). As the diameters of PS particles increased, their zeta potential increased accordingly (Fig. 1d). The zeta potential of 1000 nm PS MNPs reached 12.13 ± 0.50 mV, whereas PS MNPs diameters smaller than 100 nm (PS≤100 nm) had the lowest value (-48.23 ± 0.92 mV for 100 nm PS MNPs). PS MNPs of different diameter sizes exhibited relatively narrow hydrodynamic size distributions, with distinct peaks for each particle group and overall uniformity (Fig. 1e). Raman spectra were collected in

the range of 500 to 3500 cm^{-1}, and characteristic bands of PS MNPs were observed at 621, 1001.7, 1031.7, and 1602.7 cm^{-1} (Fig. 1f). The band at 621 cm^{-1} corresponded to the ν_{6b} radial ring-stretching mode, whereas the prominent peak at 1001.7 cm^{-1} was attributed to the ν_{12} C-CC ring bending mode. The characteristic PS MNPs band at 1031.7 cm^{-1} was assigned to the ν_{18a} tangential C-H bending mode, and the peak at 1602.7 cm^{-1} arises from the aromatic ring stretching (ν_{12}) (Lim et al., 2015). Additionally, the bands observed at 2910.2 and 3057.9 cm^{-1} were consistent with aliphatic C-H stretching and aromatic C-H stretching vibrations, respectively (Jiang et al., 2022).

3.2 Uptake and accumulation of PS MNPs in rice

The absorption and distribution of PS MNPs in rice roots were observed using a laser scanning confocal microscope and shown in Fig. 2. In the control group, noticeable fluorescence signals were observed in the epidermis along the outer ring of the root cross-section, which were attributed to the natural autofluorescence of rice tissues. No significant fluorescence signals were detected in the stele, including the xylem and phloem (Fig. 2a−c). After exposure to PS MNPs, in addition to the autofluorescence in the rice root epidermis, bright fluorescent aggregates were observed on the outer epidermal layer. Furthermore, distinct single-point fluorescence signals were detected in the xylem and phloem of the stele (Fig. 2d−u). The single-point fluorescence signals in the stele indicated that PS MNPs were absorbed by rice roots and primarily accumulated in the xylem and phloem. Driven by transpiration and supported by cohesion and adhesion, water columns in the xylem may facilitate the

upward movement of PS MNPs to aboveground tissues (Liu et al., 2022; C. Zhang et al., 2023). In addition, leaching experiment indicated that the fluorescent-labeled PS MNPs remained stable after 18 months of storage, without detectable release of fluorescent dye (Fig. S2−S3).

The concentration of PS MNPs in rice leaves was further quantified using Py-GC/MS (Fig. S4). The results indicated that rice has a certain enrichment capacity for PS MNPs, with smaller particle diameters and higher concentrations leading to greater accumulation levels. Meanwhile, no distinct PS MNPs peaks were observed in the control group. Interestingly, the mean accumulation of 100 nm PS MNPs was higher than that of 80 nm particles. Specifically, the accumulation levels of 100 nm PS MNPs reached 445 μg/g at 1 μg/mL and 701.69 μg/g at 10 μg/mL. However, no significant difference was observed between the 80 nm and 100 nm treatment groups at the same concentration.

3.3 Size-dependent effects of PS MNPs on rice quality

Protein is the second-largest storage substance in rice grains and plays a critical role in determining the eating and nutritional quality of rice, with its content influenced by environmental factors (Li et al., 2016). Rice proteins are classified into four categories based on solubility, including: water-soluble albumin, salt-soluble globulin, alcohol-soluble prolamin, and alkali-soluble glutenin (Amagliani et al., 2017). Among them, glutenin accounts for over 80% of the total endosperm protein, prolamin comprises 5%−10%, globulin 5%, and albumin 10% (Xinkang et al., 2023). In general, albumin and globulin serve as stress defense proteins (Yan et al., 2024). In this study,

albumin and globulin contents increased only when exposure to PS MNPs with particle diameters ≥800 nm (PS≥800 nm), while remaining relatively unchanged in other treatment groups (Fig. 3a−b). The change in albumin content was not statistically significant. Under exposure to PS≥800 nm, globulin content increased by 23.34% at 10 mg/kg and 28.00% at 100 mg/kg (800 nm). Prolamin content exhibited a positive correlation with PS MNPs diameter diameters (Fig. 3c), and under exposure to PS≥800 nm, it increased by 51.06% at 10 mg/kg and 48.34% at 100 mg/kg (1000 nm). PS MNPs exposure significantly reduced glutenin content, and it showed a slight increase with increasing PS MNPs diameters (Fig. 3d). Specifically, glutenin content decreased by 28.50% at 10 mg/kg (100 nm) and 24.07% at 100 mg/kg (80 nm) under PS≤100, respectively. As the most abundant protein in the endosperm, glutenin is rich in lysine and highly digestible, making it the most nutritionally valuable protein (He et al., 2021).

Rice grains contain 50%-90% starch, which serves as the primary energy storage substance (Razzaq et al., 2020). PS MNPs exposure had a negligible impact on starch content in rice, although a slight increase in grain starch content was observed with larger PS MNPs diameters (Fig. 3e). Total sugars, including soluble sugars such as glucose, fructose, and partially hydrolyzed sugars, directly affects the sweetness of rice grains. Total sugars content gradually increased with PS MNPs diameters, showing a significant rise compared to the control group (Fig. 3f). Under exposed to PS≥800 nm, total sugars content increased by 38.67% at 10 mg/kg and 38.8% at 100 mg/kg (1000 nm).

Based on the grain quality results, the effect of exposure concentrations (10 mg/kg,

100 mg/kg) was smaller than that of the PS particle diameters (80, 100, 200, 500, 800, and 1000 nm) (Table S4). Additionally, Cohen's *d* was calculated to evaluate the effect size between the PS MNPs treatment groups and the control group (Table S5). Overall, PS MNPs had a minimal effect on stress-response proteins in rice, with their levels increased only under exposed to PS≥800 nm. Meanwhile, the nutritional quality of rice grains proteins was significantly affected, with the most severe loss observed at PS≤100 nm. In contrast, PS MNPs exposure increased sugars content in rice grains, with levels gradually rising alongside particle diameters.

3.4 Size-dependent effects of PS MNPs on rice physiological properties.

ROS accumulation leads to a decline in grain quality (Suriyasak et al., 2017). Under non-stress conditions, ROS are continuously generated at basal levels in plants and are effectively scavenged by antioxidant mechanisms (enzymatic and non-enzymatic), thereby avoiding damage (Demidchik, 2015). Under stress conditions, the delicate balance between ROS production and scavenging in plants is disrupted, potentially leading to ROS accumulation in plant tissues (Wu et al., 2021) and oxidative stress (Arora. et al., 2002).

PS MNPs exposure to rice roots caused excessive ROS accumulation in rice (Fig. 4a, Fig. S5a), while ROS content gradually decreased as PS MNPs diameters increased. In leaves, exposure to PS≤100 nm resulted in a significant increase in ROS levels, reaching 25.22% at 1 μg/mL and 21.18% at 10 μg/mL (80 nm) (Fig. 4a), with other treatment groups showed minor ROS increases. In root, ROS content increased by 22.90% at 1 μg/mL (100 nm) and 22.45% at 10 μg/mL (80 nm) under PS≤100 (Fig.

323 S5a). A statistical comparison of groups with the same PS MNPs diameter but different
324 exposure concentrations (1 μg/mL and 10 μg/mL) showed that particle diameters had a
325 higher effect on ROS than concentration (Table S6). When excessive ROS accumulated,
326 rice activated a series of antioxidant strategies to sustain normal physiological functions.
327 SOD is the most critical ROS scavenger in organisms and plays a key role in
328 maintaining redox balance. Under exposure to PS MNPs, SOD activity was
329 significantly increased in rice leaves (Fig. 4b) while significantly decreased in roots
330 (Fig. S5b), indicating an impaired antioxidant capacity. In rice leaves, SOD activity
331 initially decreased and then plateaued as PS MNPs diameters increased. Under
332 exposure to PS≤100 nm, SOD activity reached a maximum increase of 74.20% at 1
333 μg/mL and 79.33% at 10 μg/mL (80 nm). In rice root, SOD activity was significantly
334 inhibited, with exposure to PS≤100 nm causing the greatest suppression, reaching 23.40%
335 at 1 μg/mL (80 nm) and 26.18% at 10 μg/mL (100 nm). POD is a heme-containing
336 enzyme that uses H_2O_2 as an electron acceptor to catalyze various oxidation reactions
337 (Passardi et al., 2005). POD activity decreased to varying degrees under PS MNPs
338 stress only in rice roots (Fig. S6). MDA, a final product of lipid peroxidation, is an
339 indicator of membrane damage (F. Huang et al., 2023). MDA content remained
340 unchanged under PS MNPs exposure (Fig. 4c, Fig. S5c), with a notable increase
341 observed only under PS≤100 nm exposure in leaves, reaching up to 38.90% at 1 μg/mL
342 and 22.98% at 10 μg/mL (100 nm) (Fig. 4c). Compared to larger particle diameters,
343 PS≤100 nm may more easily pass through and damage cell walls and membranes,
344 leading to higher levels of oxidative damage.

Soluble sugars are dissolved carbohydrates in organisms, primarily including monosaccharides and oligosaccharides such as glucose, fructose, and sucrose. These carbohydrates can act as ROS scavengers (Couee et al., 2006), with ·OH scavenging capacity ranked as sucrose > fructose > glucose (Morelli. et al., 2003). Thus, their increased content can be regarded as a stress resistance mechanism. Soluble sugars content increased with PS MNPs diameters in rice. Under exposure to PS≥800 nm, soluble sugars content in leaves increased by 55.57% at 1 μg/mL and 53.07% at 10 μg/mL (800 nm) (Fig. 4d), while in roots, it increased by 54.38% at 1 μg/mL and 42.20% at 10 μg/mL (800 nm) (Fig. S5d). Starch is an insoluble, non-structural carbohydrate composed of α-glucose polymers (Pfister & Zeeman, 2016). When degraded, it releases energy and produces sugars and their derivatives, serving as an indirect indicator of stress resistance (Wu et al., 2022; Yan et al., 2024). Starch content in rice leaves (Fig. 4e) and roots (Fig. S5e) followed the same trend, increasing with PS MNPs diameters.

Albumin and globulin serve as stress defense proteins and can provide energy reserves for plants. Under PS MNPs stress, albumin content in rice leaves (Fig. S7a) and roots (Fig. S7b) gradually decreased with increasing PS MNPs diameters. Under exposure to PS≥800 nm, albumin content in leaves declined by up to 14.23% at 1 μg/mL (800 nm) and 11.27% at 10 μg/mL (1000 nm), while in roots, the decrease reached 9.14% at 1 μg/mL and 9.65% at 10 μg/mL (800 nm). In contrast, globulin content increased with PS MNPs diameters. Under exposure to PS≥800, globulin levels in rice leaves (Fig. 4f) increased by 19.47% at 1 μg/mL and 25.09% at 10 μg/mL (1000 nm), while in roots (Fig. S5f), the increase reached 14.02% at 1 μg/mL and 10.52% at 10 μg/mL (1000 nm).

The inverse trends in albumin and globulin content with increasing PS MNPs diameters suggested an activation of stress resistance mechanisms in rice to counteract the effects of larger particles. Additionally, the rise in sugars content might have partially compensated for protein loss, contributing to the maintenance of physiological and biochemical balance in rice. Under PS MNPs exposure, prolamin content in rice increased with PS MNPs size, while glutenin content showed no significant changes (Fig. S9). Under exposure to PS≥800 nm, prolamin content in rice leaves (Fig. S8a) increased by 17.06% at 1 μg/mL and 22.69% at 10 μg/mL (1000 nm), while in roots (Fig. S8b), the increase reached 16.08% and 28.68%, respectively.

Overall, the impact of exposure concentrations (1 μg/mL, 10 μg/mL) was smaller than that of the PS MNPs particle diameters (80, 100, 200, 500, 800, and 1000 nm) (Table S6). Cohen's *d* was also calculated to quantify the effect size between the PS MNPs treatment groups and the control group (Table S7-S8). Exposure of rice roots to PS MNPs induced ROS accumulation, and roots experiencd greater oxidative damage than the leaves, disrupting intracellular redox balance. In response to excessive ROS, rice modulated the activities of SOD and POD. As PS MNPs diameters increased, rice enhanced the levels of soluble sugars, sucrose, and globulin, alleviating PS MNPs stress while reducing plant damage.

3.5 Impact of PS MNPs on the global metabolic network in rice

To further elucidate the mechanisms by which PS MNPs affected rice physiology, we conducted metabolomics analysis to examine the variation of final products of genome-environment interaction. Since the effects of PS MNPs exposure

389 concentrations (1 μg/mL, 10 μg/mL) on rice physiology was minimal, we selected 1
390 μg/mL PS MNPs treatment group for further metabolic analysis.

391 Principal component analysis (PCA) was performed to determine metabolic
392 difference among PS-treated and control groups. As illustrated in Fig. 5a–b, PC1 and
393 PC2 cumulatively explained 55.3% and 76.2% of the metabolic variation in leaves and
394 roots, respectively. Totally, 131 metabolites in leaves and 74 in roots were identified
395 using an LC-MS/MS system (Fig. 5c–d). Based on the selection criteria (P< 0.05, -1 <
396 $\log_2$ (fold change) < 1), differentially expressed metabolites (DEMs) in leaves and roots
397 under exposure to PS MNPs of different diameters were identified. As shown in Fig.
398 S10–S11, more than 60% of the identified DEMs were upregulated. The DEMs were
399 subjected to KEGG pathway analysis, and the top 15 significantly perturbed pathways
400 were selected according to pathway impact and P-value. Fig. S12 showed that the
401 significantly perturbed pathways in rice leaves across treatments were similar,
402 predominantly involving carbohydrate metabolism and a similar trend was observed in
403 roots (Fig. S13). Nine significantly perturbed metabolic pathways shared among
404 treatment groups were identified. The relative proportion of each significantly disturbed
405 metabolic pathway was assessed, in which carbohydrate metabolism being the most
406 prominent, followed by amino acid metabolism (Fig. S14). The perturbation levels of
407 12 carbohydrate metabolism pathways were further assessed, with galactose
408 metabolism showing the highest disturbance (Fig. S15).

409 Six metabolites involved with galactose metabolism pathway were identified in
410 leaves, and three related metabolites were detected in roots. Interestingly, the relative

411 abundance of the six metabolites detected in leaves was generally upregulated (Table
412 S9), while the abundance of the three metabolites detected in roots was downregulated
413 (Table S10). Most metabolites in plant galactose metabolism, such as galactose,
414 galactitol, act as non-enzymatic antioxidants, scavenging ROS and enhancing plant
415 tolerance to exogenous stress (Bolouri-Moghaddam et al., 2010). Exposure to PS
416 nanoplastics induced the upregulation of galactose metabolism in crops, which not only
417 improved stress tolerance but also met the demands of energy metabolism (Lian et al.,
418 2020). As amino acid metabolism is the second most disturbed metabolic pathway, we
419 further analyzed the amino acids obtained from rice leaves and roots using cluster
420 analysis (Fig. S16−17). Similar to soluble small molecule sugars, amino acids play a
421 significant role in plant development and stress defense (Trovato et al., 2021). Under
422 PS MNPs exposure, most amino acids detected in the leaves were upregulated, whereas
423 the majority in the roots were downregulated. PS MNPs exposure induced a high level
424 of oxidative stress in rice. To maintain normal physiological and biochemical functions,
425 rice upregulated carbohydrate and amino acid metabolism pathway to alleviate
426 oxidative stress.

427 **3.6 The size-dependent effects of PS MNPs on rice metabolism**

428 To further investigate the size-dependent effects of PS MNPs exposure on rice
429 metabolism and uncover the metabolic mechanisms underlying grain quality changes,
430 a weighted gene co-expression network analysis (WGCNA) was performed to identify
431 metabolites highly correlated with exposure diameters based on differentially expressed
432 metabolites. In leaves, the top seven metabolites with the highest interaction degree

were fructose 6-phosphate, glucose 6-phosphate, ribitol, xylitol, arabitol, lysine, and isopentenyl pyrophosphate (Fig. 5f). In roots, the top four metabolites with the highest interaction degree were citrate, lyxose, malate, and mannose 6-phosphate (Fig. 5e).

Metabolic network diagrams were constructed to visualize the changes in metabolites highly correlated with PS MNPs diameter size (Fig. 6). The metabolites identified in leaves were primarily positively correlated with PS MNPs diameters and were enriched in glycolysis/gluconeogenesis, pentose and glucuronate interconversions (Fig. 6a). With increasing PS MNPs diameters , rice progressively activated the pentose and glucuronate interconversion pathway in leaves, as evidenced by the rising relative abundances of xylitol, D-arabitol, ribitol, and D-glucuronate. However, this upward trend plateaued when PS MNPs diameters exceeded 800 nm. The accumulation of sugars alcohols enhanced plant stress tolerance and played a key role in coping with PS MNPs stress (Ozturk et al., 2021). Under exposure to 100 nm polyamide (PA), the pentose and glucuronate interconversion pathway in rice was upregulated, with increased relative abundance of D-arabinose (Yang et al., 2024). Similarly, Huang et al. (D. Huang et al., 2023) reported that when cucumber (*Cucumis sativus*) leaves were exposed to diameters of 50–100 nm polystyrene (PS) particles three weeks, the pentose and glucuronate interconversion pathway was upregulated, indicating that carbohydrate metabolic reprogramming enhanced the plant's tolerance to PS-induced stress.

The relative abundance of upstream glycolysis/gluconeogenesis metabolites D-glucose-6P and D-fructose-6P were negatively correlated with PS MNPs diameters, while the downstream metabolites glycerate-3P and glycerate-2P showed a positive

455 correlation. When the PS MNPs diameters exceeded 800 nm, the abundance of D-
456 glucose-6P and D-fructose-6P significantly decreased, while the abundance of
457 glycerate-3P and glycerate-2P also declined, revealing a contradiction between the
458 relative abundances of upstream and downstream metabolites. Fructose-bisphosphate
459 aldolase (FBA), a key enzyme in glycolysis/gluconeogenesis, catalyzes the cleavage of
460 fructose-1,6-bisphosphate into two three-carbon molecules, including glyceraldehyde-
461 3-phosphate (GAP) and dihydroxyacetone phosphate. GAP was further converted into
462 glycerate-3P (3-PGA) and glycerate-2P (2-PGA) through enzymatic reactions, making
463 FBA a critical link between upstream metabolites (D-glucose-6P, D-fructose-6P) and
464 downstream metabolites (glycerate-3P, glycerate-2P). Under PS MNPs exposure, FBA
465 activity gradually decreased with increasing PS MNPs diameters (Fig. S18). Under
466 exposure to PS≥800 nm, FBA activity in rice leaves was suppressed by 50.92% at 1
467 μg/mL and 45.43% at 10 μg/mL (1000 nm). The reduced availability of upstream
468 substrates constrained glycolytic flux, and the concomitant decline in FBA activity
469 represented a passive response to substrate scarcity. When FBA activity declined, the
470 levels of 3-phosphoglycerate (3-PGA) and 2-phosphoglycerate (2-PGA) increased,
471 suggesting that their accumulation was primarily due to inhibited downstream
472 utilization rather than impaired production. Prolonged accumulation of 3-PGA and 2-
473 PGA could have exerted feedback inhibition on upstream phosphatase enzymes, further
474 weakening the phosphorylation-dependent breakdown of photosynthetic products. This,
475 in turn, indirectly reduced the efficiency of carbohydrate catabolism and promotes
476 sugars accumulation. In one study, 14-day exposure to 100 nm PS regulated aldolase

activity in wheat leaves and roots, restructuring carbohydrate metabolism to mitigate the adverse effects of PS on wheat (S. Li et al., 2021). In rice leaves, the relative abundance of succinate, a key TCA cycle intermediate, significantly increased under exposure to PS MNPs larger than 100 nm, reflecting heightened energy demands. Lysine is the first limiting essential amino acid in gramineous crops (Galili, 2002). With increasing particle diameters of PS MPs, the lysine content in rice leaves gradually increased, whereas the glutamic acid decreased progressively (Fig. 5, Fig. S16). Glutamic acid is a key precursor for glutelin synthesis and one of its most abundant amino acids. It also played a crucial role in antioxidant defense by participating in the γ-aminobutyric acid (GABA) metabolic pathway, thereby indirectly reducing the accumulation of ROS in rice. Under exposure to PS≤100 nm, although glutamic acid content in leaves remained relatively high, the glutelin content in grains was comparatively low, suggesting that glutamic acid was more involved in antioxidant processes and less available for protein synthesis. As particle diameters increased, glutamic acid content gradually decreased. However, enhanced defense responses at larger particle diameters might have redirected more glutamic acid toward glutelin synthesis, resulting in a moderate increase in glutelin content.

The metabolites identified in roots were primarily negatively correlated with PS MNPs diameters, and the DEM were mainly enriched in fructose and mannose metabolism (Fig. 6b). Relative abundances of several metabolites in the fructose and mannose metabolism pathway, such as L-sorbose, D-sorbitol, D-mannitol, and D-mannose-6P, gradually decrease with increasing PS MNPs diameters. When PS MNPs

diameters exceeded 100 nm, the decline in fructose and mannose metabolism became more significant in roots, potentially reducing the capacity to resist osmotic stress and disrupting osmotic balance.

4. Conclusion

This study demonstrated that PS MNPs deteriorated the protein nutrition in rice grains and exhibited a size-dependent effect by affecting metabolism. PS MNPs exposure induced a significant decline of glutenin content in rice grains, especially for PS≤100 nm exposure. As the PS MNPs diameters increased, the extent of glutenin depletion decreased, while starch and sugars accumulation progressively rose. Hydroponic experiment demonstrated that PS MNPs were absorbed by rice roots, and it primarily accumulated in xylem and phloem. Driven by transpiration pull, PS was transported upward, potentially affecting rice physiology, metabolism, and grain quality. The content of starch, soluble sugars, xylitol, D-arabitol, and ribitol were increased with the particle diameter of PS MNPs in the range of 80–800 nm. Simultaneously, the TCA cycle in leaves was progressively activated, and glycolysis/gluconeogenesis was modulated, with the significant inhibition of the key enzyme FBA. Compared to leaves, roots exhibited a more pronounced PS-induced stress response. Notably, PS≤100 nm imposed the highest biotoxicity and the most detrimental impact on grain quality, whereas PS≥800 nm triggered an enhanced defense response, improving rice resilience to external stress. Polystyrene exhibited high chemical stability (Ho et al., 2018) and was unlikely to degrade within rice tissues, thus the observed impacts on rice were primarily attributed to the physical properties of MNPs, such as particle diameter, and

MPs of varied composition might have exerted comparable effects on plants. Therefore, special attention should be paid to the potential risks posed by small-diameters (≤100 nm) MNPs exposure towards rice.

Author Information

Corresponding Author

Wei Wang – College of Environmental and Resource Sciences, Zhejiang University, Hangzhou, Zhejiang 310058, China; Zhejiang Provincial Key Laboratory of Organic Pollution Process and Control, Hangzhou, Zhejiang 310058, China; email: ww1@zju.edu.cn

Authors

Xiangrui Miao – College of Environmental and Resource Sciences, Zhejiang University, Hangzhou, Zhejiang 310058, China; Zhejiang Provincial Key Laboratory of Organic Pollution Process and Control, Hangzhou, Zhejiang 310058, China

Lizhong Zhu – College of Environmental and Resource Sciences, Zhejiang University, Hangzhou, Zhejiang 310058, China; Zhejiang Provincial Key Laboratory of Organic Pollution Process and Control, Hangzhou, Zhejiang 310058, China

CRediT authorship contribution statement

Xiangrui Miao： Conceptualization, Data curation, Investigation, Methodology, Software, Visualization, Writing – original draft. **Wei wang:** Writing – review & editing, Supervision, Funding acquisition. **Lizhong Zhu:** Writing – review & editing, Funding acquisition, Project administration, Resources, Supervision**.**

Declaration of Competing Interest

The authors declare that they have no know competing financial interests or personal relationships that could have appeared to influence the work reported in this paper.

Data availability

Data will be made available on request.

Acknowledgements

This work was financially supported by the Natural Science Foundation of China (NO. 22436006) and the National Key Research and Development Program of China (NO. 2023YFC3708101). Additionally, the authors are grateful to Yunqin Li in Analysis Center of Agrobiology and Environmental Sciences (ACAES) of Zhejiang University for her help with LSCM measurements and WeiKang Zhang in department of chemistry of Zhejiang University for his help with Raman measurements.

Appendix A. Supporting information

Supplementary data associated with this article includes 7 texts, 10 tables and 18 figures.

558 **References**

559 Amagliani, L., O'Regan, J., Kelly, A. L., & O'Mahony, J. A. (2017). The composition,
560 extraction, functionality and applications of rice proteins: A review. Trends in Food
561 Science & Technology, 64, 1-12. https://doi.org/10.1016/j.tifs.2017.01.008

562 Arora., A., Sairam., R. K., & Srivastava., G. C. (2002). Oxidative stress and
563 antioxidative system in plants. Curr. Sci, 82, 1227-1238.
564 https://doi.org/10.1111/pce.12726

565 Asad, M., Khan, Z., Shah, T., Shah, M. A., Imran, A., Rasool, S., Khattak, J. Z. K.,
566 Khan, S. R., Ahmad, A., & Ahmad, P. (2024). Mitigation of microplastic toxicity in
567 soybean by synthetic bacterial community and arbuscular mycorrhizal fungi interaction:
568 Altering carbohydrate metabolism, hormonal transduction, and genes associated with
569 lipid and protein metabolism. Plant Stress, 14.
570 https://doi.org/10.1016/j.stress.2024.100631

571 Bolouri-Moghaddam, M. R., Le Roy, K., Xiang, L., Rolland, F., & Van den Ende, W.
572 (2010). Sugar signalling and antioxidant network connections in plant cells. FEBS J,
573 277(9), 2022-2037. https://doi.org/10.1111/j.1742-4658.2010.07633.x

574 Charles, B., & Irwin, F. (1971). Superoxide dismutase: Improved assays and an assay
575 applicable to acrylamide gels. Anal. Biochem, 44, 276-287.
576 https://doi.org/10.1016/0003-2697(71)90370-8

577 Chen, J., Le, X. C., & Zhu, L. (2019). Metabolomics and transcriptomics reveal defense
578 mechanism of rice (*Oryza sativa*) grains under stress of 2,2',4,4'-tetrabromodiphenyl
579 ether. Environ Int, 133(Pt A), 105154. https://doi.org/10.1016/j.envint.2019.105154

Chen, S., Feng, Y., Han, L., Li, D., Feng, Y., Jeyakumar, P., Sun, H., Shi, W., & Wang, H. (2022). Responses of rice *(Oryza sativa* L.) plant growth, grain yield and quality, and soil properties to the microplastic occurrence in paddy soil. Journal of Soils and Sediments, 22(8), 2174-2183. https://doi.org/10.1007/s11368-022-03232-w

Couee, I., Sulmon, C., Gouesbet, G., & El Amrani, A. (2006). Involvement of soluble sugars in reactive oxygen species balance and responses to oxidative stress in plants. J Exp Bot, 57(3), 449-459. https://doi.org/10.1093/jxb/erj027

Demidchik, V. (2015). Mechanisms of oxidative stress in plants: From classical chemistry to cell biology. Environmental and Experimental Botany, 109, 212-228. https://doi.org/10.1016/j.envexpbot.2014.06.021

Galili, G. (2002). New insights into the regulation and functional significance of lysine metabolism in plants. Annu Rev Plant Biol, 53, 27-43. https://doi.org/10.1146/annurev.arplant.53.091401.110929

Hasan, M. M., & Tarannum, M. N. (2025). Adverse impacts of microplastics on soil physicochemical properties and crop health in agricultural systems. Journal of Hazardous Materials Advances, 17. https://doi.org/10.1016/j.hazadv.2024.100528

He, W., Wang, L., Lin, Q., & Yu, F. (2021). Rice seed storage proteins: Biosynthetic pathways and the effects of environmental factors. J Integr Plant Biol, 63(12), 1999-2019. https://doi.org/10.1111/jipb.13176

He, X., Wang, Q., Qian, Y., Li, Z., & Feng, C. (2024). Microplastic accumulation and oxidative stress in sweet pepper (*Capsicum annuum* Linn.): Role of the size effect. Environ Pollut, 360, 124652. https://doi.org/10.1016/j.envpol.2024.124652

602 Ho, B. T., Roberts, T. K., & Lucas, S. (2018). An overview on biodegradation of
603 polystyrene and modified polystyrene: the microbial approach. Crit Rev Biotechnol,
604 38(2), 308-320. https://doi.org/10.1080/07388551.2017.1355293
605 Huang, D., Shi, Z., Shan, X., Yang, S., Zhang, Y., & Guo, X. (2023). Insights into
606 growth-affecting effect of nanomaterials: Using metabolomics and transcriptomics to
607 reveal the molecular mechanisms of cucumber leaves upon exposure to polystyrene
608 nanoplastics (PSNPs). Sci Total Environ, 866, 161247.
609 https://doi.org/10.1016/j.scitotenv.2022.161247
610 Huang, F., Hu, J., Chen, L., Wang, Z., Sun, S., Zhang, W., Jiang, H., Luo, Y., Wang, L.,
611 Zeng, Y., & Fang, L. (2023). Microplastics may increase the environmental risks of Cd
612 via promoting Cd uptake by plants: A meta-analysis. J Hazard Mater, 448, 130887.
613 https://doi.org/10.1016/j.jhazmat.2023.130887
614 Jamil, A., Ahmad, A., Moeen-Ud-Din, M., Zhang, Y., Zhao, Y., Chen, X., Cui, X., Tong,
615 Y., & Liu, X. (2025). Unveiling the mechanism of micro-and-nano plastic phytotoxicity
616 on terrestrial plants: A comprehensive review of omics approaches. Environ Int, 195,
617 109257. https://doi.org/10.1016/j.envint.2025.109257
618 Jiang, M., Wang, B., Ye, R., Yu, N., Xie, Z., Hua, Y., Zhou, R., Tian, B., & Dai, S.
619 (2022). Evidence and Impacts of Nanoplastic Accumulation on Crop Grains. Adv Sci
620 (Weinh), 9(33), e2202336. https://doi.org/10.1002/advs.202202336
621 Jiang, X., Chen, H., Liao, Y., Ye, Z., Li, M., & Klobucar, G. (2019). Ecotoxicity and
622 genotoxicity of polystyrene microplastics on higher plant Vicia faba. Environ Pollut,
623 250, 831-838. https://doi.org/10.1016/j.envpol.2019.04.055

624 Jin, T., Tang, J., Lyu, H., Wang, L., Gillmore, A. B., & Schaeffer, S. M. (2022).
625 Activities of Microplastics (MPs) in Agricultural Soil: A Review of MPs Pollution from
626 the Perspective of Agricultural Ecosystems. J Agric Food Chem, 70(14), 4182-4201.
627 https://doi.org/10.1021/acs.jafc.1c07849
628 Keunen, E., Peshev, D., Vangronsveld, J., Van Den Ende, W., & Cuypers, A. (2013).
629 Plant sugars are crucial players in the oxidative challenge during abiotic stress:
630 extending the traditional concept. Plant Cell Environ, 36(7), 1242-1255.
631 https://doi.org/10.1111/pce.12061
632 Kik, K., Bukowska, B., & Sicinska, P. (2020). Polystyrene nanoparticles: Sources,
633 occurrence in the environment, distribution in tissues, accumulation and toxicity to
634 various organisms. Environ Pollut, 262, 114297.
635 https://doi.org/10.1016/j.envpol.2020.114297
636 Li, C., Gao, Y., He, S., Chi, H.-Y., Li, Z.-C., Zhou, X.-X., & Yan, B. (2021).
637 Quantification of Nanoplastic Uptake in Cucumber Plants by Pyrolysis Gas
638 Chromatography/Mass Spectrometry. Environmental Science & Technology Letters,
639 8(8), 633-638. https://doi.org/10.1021/acs.estlett.1c00369
640 Li, G.-h., Chen, Y.-l., Ding, Y.-f., Geng, C.-m., Li, Q., Liu, Z.-h., Wang, S.-h., & Tang,
641 S. (2016). Charactering protein fraction concentrations as influenced by nitrogen
642 application in low-glutelin rice cultivars. Journal of Integrative Agriculture, 15(3), 537-
643 544. https://doi.org/10.1016/s2095-3119(15)61182-0
644 Li, L., Luo, Y., Li, R., Zhou, Q., Peijnenburg, W. J. G. M., Yin, N., Yang, J., Tu, C., &
645 Zhang, Y. (2020). Effective uptake of submicrometre plastics by crop plants via a crack-

entry mode. Nature Sustainability, 3(11), 929-937. https://doi.org/10.1038/s41893-020-0567-9

Li, L., Zhou, Q., Yin, N., Tu, C., & Luo, Y. (2019). Uptake and accumulation of microplastics in an edible plant. Chinese Science Bulletin, 64(9), 928-934. https://doi.org/10.1360/n972018-00845

Li, R., Li, L., Zhang, Y., Yang, J., Tu, C., Zhou, Q., Li, Y., & Luo, Y. (2020). Uptake and accumulation of microplastics in a cereal plant wheat. Chin Sci Bull, 65(20), 2120-2127. https://doi.org/10.1360/tb-2020-0030

Li, S., Guo, J., Wang, T., Gong, L., Liu, F., Brestic, M., Liu, S., Song, F., & Li, X. (2021). Melatonin reduces nanoplastic uptake, translocation, and toxicity in wheat. J Pineal Res, 71(3), e12761. https://doi.org/10.1111/jpi.12761

Li, Z., Li, R., Li, Q., Zhou, J., & Wang, G. (2020). Physiological response of cucumber (*Cucumis sativus* L.) leaves to polystyrene nanoplastics pollution. Chemosphere, 255, 127041. https://doi.org/10.1016/j.chemosphere.2020.127041

Lian, J., Wu, J., Xiong, H., Zeb, A., Yang, T., Su, X., Su, L., & Liu, W. (2020). Impact of polystyrene nanoplastics (PSNPs) on seed germination and seedling growth of wheat (*Triticum aestivum* L.). J Hazard Mater, 385, 121620. https://doi.org/10.1016/j.jhazmat.2019.121620

Lim, J. Y., Nam, J. S., Yang, S. E., Shin, H., Jang, Y. H., Bae, G. U., Kang, T., Lim, K. I., & Choi, Y. (2015). Identification of Newly Emerging Influenza Viruses by Surface-Enhanced Raman Spectroscopy. Anal Chem, 87(23), 11652-11659. https://doi.org/10.1021/acs.analchem.5b02661

668 Liu, Y., Guo, R., Zhang, S., Sun, Y., & Wang, F. (2022). Uptake and translocation of
669 nano/microplastics by rice seedlings: Evidence from a hydroponic experiment. J
670 Hazard Mater, 421, 126700. https://doi.org/10.1016/j.jhazmat.2021.126700
671 Ma, J., Aqeel, M., Khalid, N., Nazir, A., Alzuaibr, F. M., Al-Mushhin, A. A. M., Hakami,
672 O., Iqbal, M. F., Chen, F., Alamri, S., Hashem, M., & Noman, A. (2022). Effects of
673 microplastics on growth and metabolism of rice (*Oryza sativa* L.). Chemosphere,
674 307(Pt 1), 135749. https://doi.org/10.1016/j.chemosphere.2022.135749
675 Morelli., R., Russo-Volpe., S., Bruno., N., & Scalzo., R. L. (2003). Fenton-dependent
676 damage to carbohydrates: Free radical scavenging activity of some simple sugars
677 J.Agric.Food Chem., 51, 7418-7425.
678 Ozturk, M., Turkyilmaz Unal, B., Garcia-Caparros, P., Khursheed, A., Gul, A., &
679 Hasanuzzaman, M. (2021). Osmoregulation and its actions during the drought stress in
680 plants. Physiol Plant, 172(2), 1321-1335. https://doi.org/10.1111/ppl.13297
681 Paliwal, A., Laborte, A., Nelson, A., & Singh, R. K. (2018). Salinity stress detection in
682 rice crops using time series MODIS VI data. International Journal of Remote Sensing,
683 40(21), 8186-8202. https://doi.org/10.1080/01431161.2018.1513667
684 Passardi, F., Cosio, C., Penel, C., & Dunand, C. (2005). Peroxidases have more
685 functions than a Swiss army knife. Plant Cell Rep, 24(5), 255-265.
686 https://doi.org/10.1007/s00299-005-0972-6
687 Pfister, B., & Zeeman, S. C. (2016). Formation of starch in plant cells. Cell Mol Life
688 Sci, 73(14), 2781-2807. https://doi.org/10.1007/s00018-016-2250-x
689 Q, Y., & Z, R. (1999). Drought and salinity differentially influence activities of

690 superoxide dismutases in narrow-leafed lupins. Plant Sci, 142, 1-11.
691 https://doi.org/10.1016/S0168-9452(98)00246-5
692 Qi, R., Jones, D. L., Li, Z., Liu, Q., & Yan, C. (2020). Behavior of microplastics and
693 plastic film residues in the soil environment: A critical review. Sci Total Environ, 703,
694 134722. https://doi.org/10.1016/j.scitotenv.2019.134722
695 Razzaq, A., Ali, A., Safdar, L. B., Zafar, M. M., Rui, Y., Shakeel, A., Shaukat, A., Ashraf,
696 M., Gong, W., & Yuan, Y. (2020). Salt stress induces physiochemical alterations in rice
697 grain composition and quality. J Food Sci, 85(1), 14-20. https://doi.org/10.1111/1750-
698 3841.14983
699 Rillig, M. C., Kim, S. W., & Zhu, Y. G. (2024). The soil plastisphere. Nat Rev Microbiol,
700 22(2), 64-74. https://doi.org/10.1038/s41579-023-00967-2
701 Shi, X., Shi, R., Fu, X., Zhao, Y., Ge, Y., Liu, J., Chen, C., & Liu, W. (2024). Impact of
702 microplastics on plant physiology: A meta-analysis of dose, particle size, and crop type
703 interactions in agricultural ecosystems. Sci Total Environ, 955, 177245.
704 https://doi.org/10.1016/j.scitotenv.2024.177245
705 Suriyasak, C., Harano, K., Tanamachi, K., Matsuo, K., Tamada, A., Iwaya-Inoue, M.,
706 & Ishibashi, Y. (2017). Reactive oxygen species induced by heat stress during grain
707 filling of rice (*Oryza sativa* L.) are involved in occurrence of grain chalkiness. J Plant
708 Physiol, 216, 52-57. https://doi.org/10.1016/j.jplph.2017.05.015
709 Thompson., R. C., Olsen., Y., Mitchell., R. P., & Davis., A. (2004). Lost at sea: Where
710 is all the plastic? Science, 304, 838.
711 Trovato, M., Funck, D., Forlani, G., Okumoto, S., & Amir, R. (2021). Editorial: Amino

712 Acids in Plants: Regulation and Functions in Development and Stress Defense. Front
713 Plant Sci, 12, 772810. https://doi.org/10.3389/fpls.2021.772810
714 Weithmann, N., N.Moller, J., G.J.Loder, M., & Piehl, S. (2018). Organic fertilizer as a
715 vehicle for the entry of microplastic into the environment. Sci.Adv, 4, 8060.
716 https://doi.org/10.1126/sciadv.aap806
717 Wu, J., Liu, W., Zeb, A., Lian, J., Sun, Y., & Sun, H. (2021). Polystyrene microplastic
718 interaction with *Oryza sativa*: toxicity and metabolic mechanism. Environmental
719 Science: Nano, 8(12), 3699-3710. https://doi.org/10.1039/d1en00636c
720 Wu, X., Hou, H., Liu, Y., Yin, S., Bian, S., Liang, S., Wan, C., Yuan, S., Xiao, K., Liu,
721 B., Hu, J., & Yang, J. (2022). Microplastics affect rice (*Oryza sativa* L.) quality by
722 interfering metabolite accumulation and energy expenditure pathways: A field study. J
723 Hazard Mater, 422, 126834. https://doi.org/10.1016/j.jhazmat.2021.126834
724 Xinkang, L., Chunmin, G., Lin, W., Liting, J., Xiangjin, F., Qinlu, L., Zhengyu, H., &
725 Chun, L. (2023). Rice Storage Proteins: Focus on Composition, Distribution, Genetic
726 Improvement and Effects on Rice Quality. Rice Science, 30(3), 207-221.
727 https://doi.org/10.1016/j.rsci.2023.03.005
728 Yan, Y., Yang, H., Du, Y., Li, X., & Li, X. (2024). Effects and molecular mechanisms
729 of polyethylene microplastic oxidation on wheat grain quality. J Hazard Mater, 474,
730 134816. https://doi.org/10.1016/j.jhazmat.2024.134816
731 Yang, L., Luo, L., Cai, W., Chen, Z., Luo, X., & Chen, Y. (2024). Changes in
732 carbohydrate metabolism and soil microorganisms under the stress of polyamide and
733 polyethylene nanoplastics during rice (*Oryza sativa* L.) growth. Sci Total Environ, 912,

734 169183. https://doi.org/10.1016/j.scitotenv.2023.169183

735 Yao, X., Lin, Z., Chen, W., Pan, Z., Hou, L., Li, J., Li, D., Liu, W., & Hu, K. (2024).
736 Toxic effects of microplastics (MPs) on aquatic plants and phytoremediation potential
737 in freshwater environments. Journal of Water Process Engineering, 68.
738 https://doi.org/10.1016/j.jwpe.2024.106485

739 Zhang, C., Yue, N., Li, X., Shao, H., Wang, J., An, L., & Jin, F. (2023). Potential
740 translocation process and effects of polystyrene microplastics on strawberry seedlings.
741 Journal of Hazardous Materials, 449. https://doi.org/10.1016/j.jhazmat.2023.131019

742 Zhang, Q., Zhao, M., Meng, F., Xiao, Y., Dai, W., & Luan, Y. (2021). Effect of
743 Polystyrene Microplastics on Rice Seed Germination and Antioxidant Enzyme Activity.
744 Toxics, 9(8). https://doi.org/10.3390/toxics9080179

745 Zhang, Y., Tian, X., Huang, P., Yu, X., Xiang, Q., Zhang, L., Gao, X., Chen, Q., & Gu,
746 Y. (2023). Biochemical and transcriptomic responses of buckwheat to polyethylene
747 microplastics. Sci Total Environ, 899, 165587.
748 https://doi.org/10.1016/j.scitotenv.2023.165587

749 Zhou, C. Q., Lu, C. H., Mai, L., Bao, L. J., Liu, L. Y., & Zeng, E. Y. (2021). Response
750 of rice (*Oryza sativa* L.) roots to nanoplastic treatment at seedling stage. J Hazard Mater,
751 401, 123412. https://doi.org/10.1016/j.jhazmat.2020.123412

752 Zhu, J., Wang, J., Chen, R., Feng, Q., & Zhan, X. (2022). Cellular Process of
753 Polystyrene Nanoparticles Entry into Wheat Roots. Environ Sci Technol, 56(10), 6436-
754 6444. https://doi.org/10.1021/acs.est.1c08503

755 Zhu, W., Lu, S., Jiang, H., Wang, P., He, C., Bian, H., & Wang, J. (2023). Interactions

between phenanthrene and polystyrene micro/nano plastics: Implications for rice (*Oryza sativa* L.) toxicity. Environ Pollut, 337, 122360. https://doi.org/10.1016/j.envpol.2023.122360

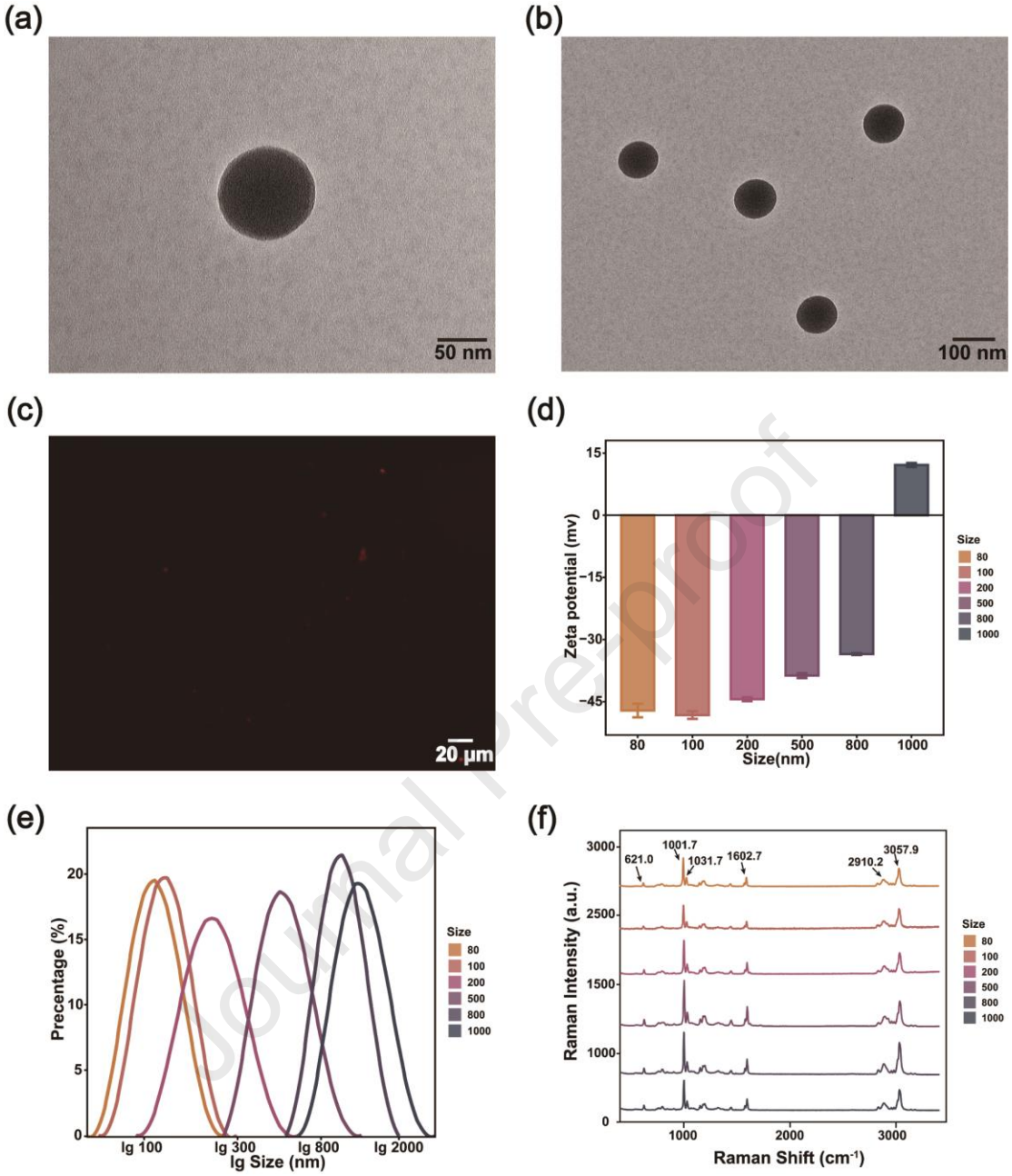

Figure 1. Analytical characterization analysis of polystyrene microplastics, including TEM morphological analysis of 80 nm polystyrene at scale bar of 50 nm (a) and 100 nm (b), fluorescence images at scale bar of 20 μm (c), zeta potential in pure water at 25°C and pH 7.0 (d), the hydrodynamic diameter in pure water at 25°C and pH 7.0 (e), and Raman spectra of polystyrene (f).

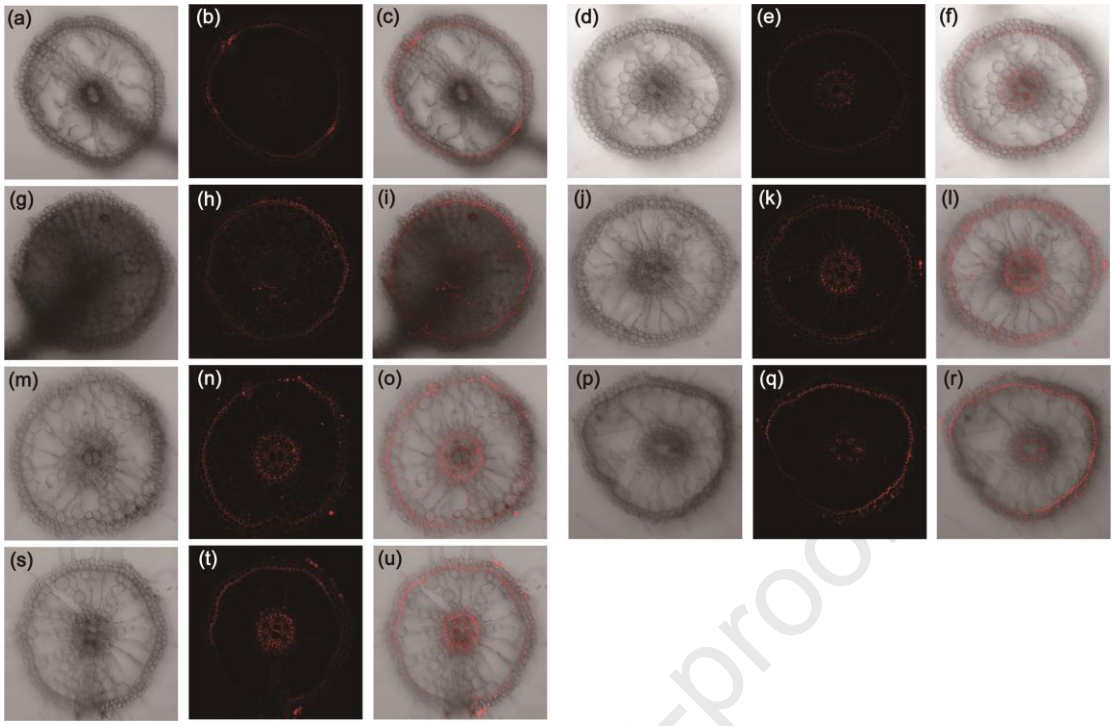

Figure 2. Confocal characterization images of rice root cross-sections after 14 days of hydroponic exposure to 1 μg/mL PS MNPs in the groups of control group (a−c), 80 nm (d−f), 100 nm (g−i), 200 nm (j−l), 500 nm (m−o), 800 nm (p−r), 1000 nm (s−u). Every three images form a group, arranged from left to right as: bright field, fluorescence, and merged.

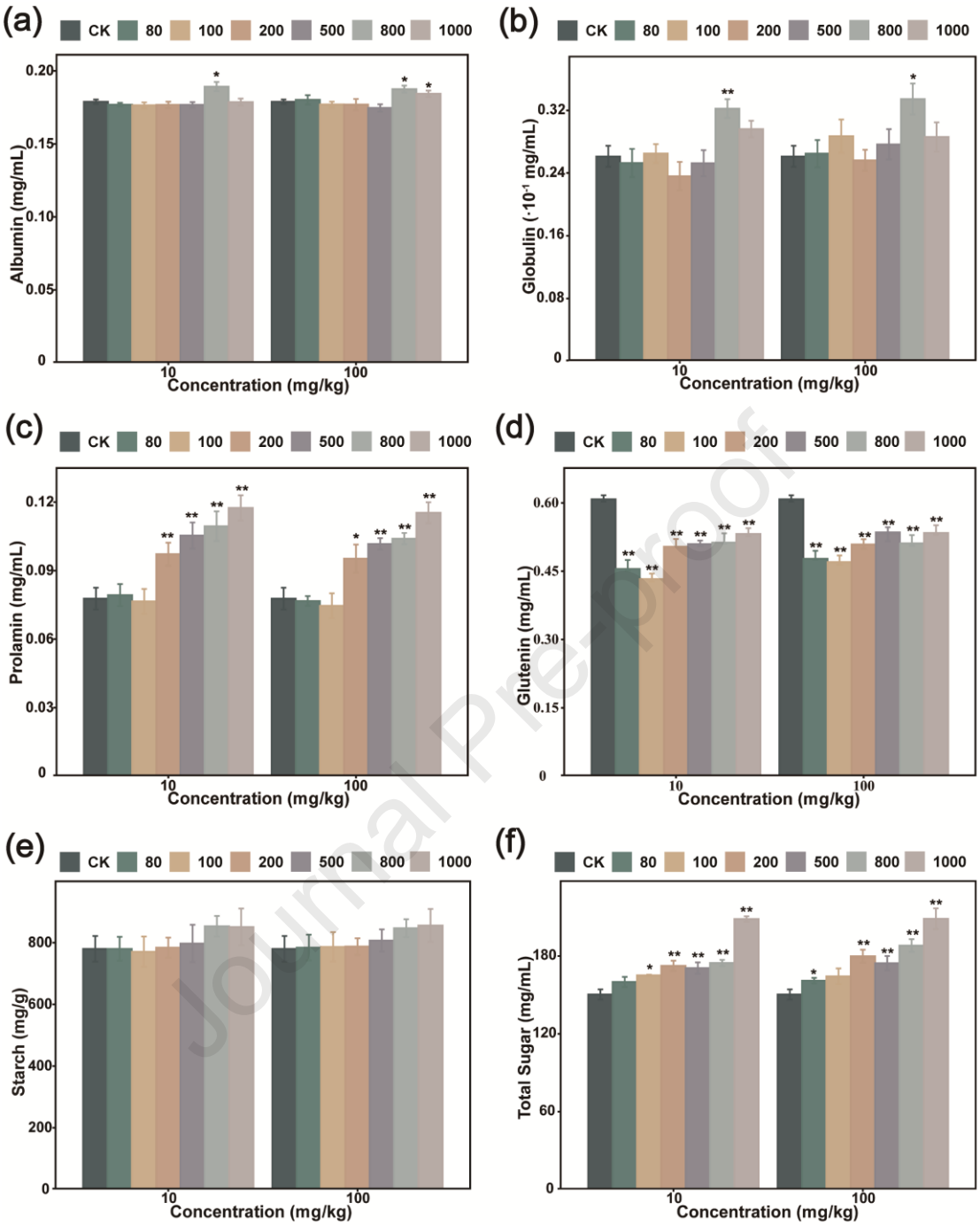

Figure 3. Content of albumin (a), globulin (b), prolamin (c), glutelin (d), starch (e) and total sugar(f) in rice grains after 180 days of exposure to polystyrene microplastics. For a given PS particle diameter and concentration, significant differences between the control and treatment groups (intergroup comparsion) are marked with * ($P < 0.05$) and ** ($P < 0.01$).

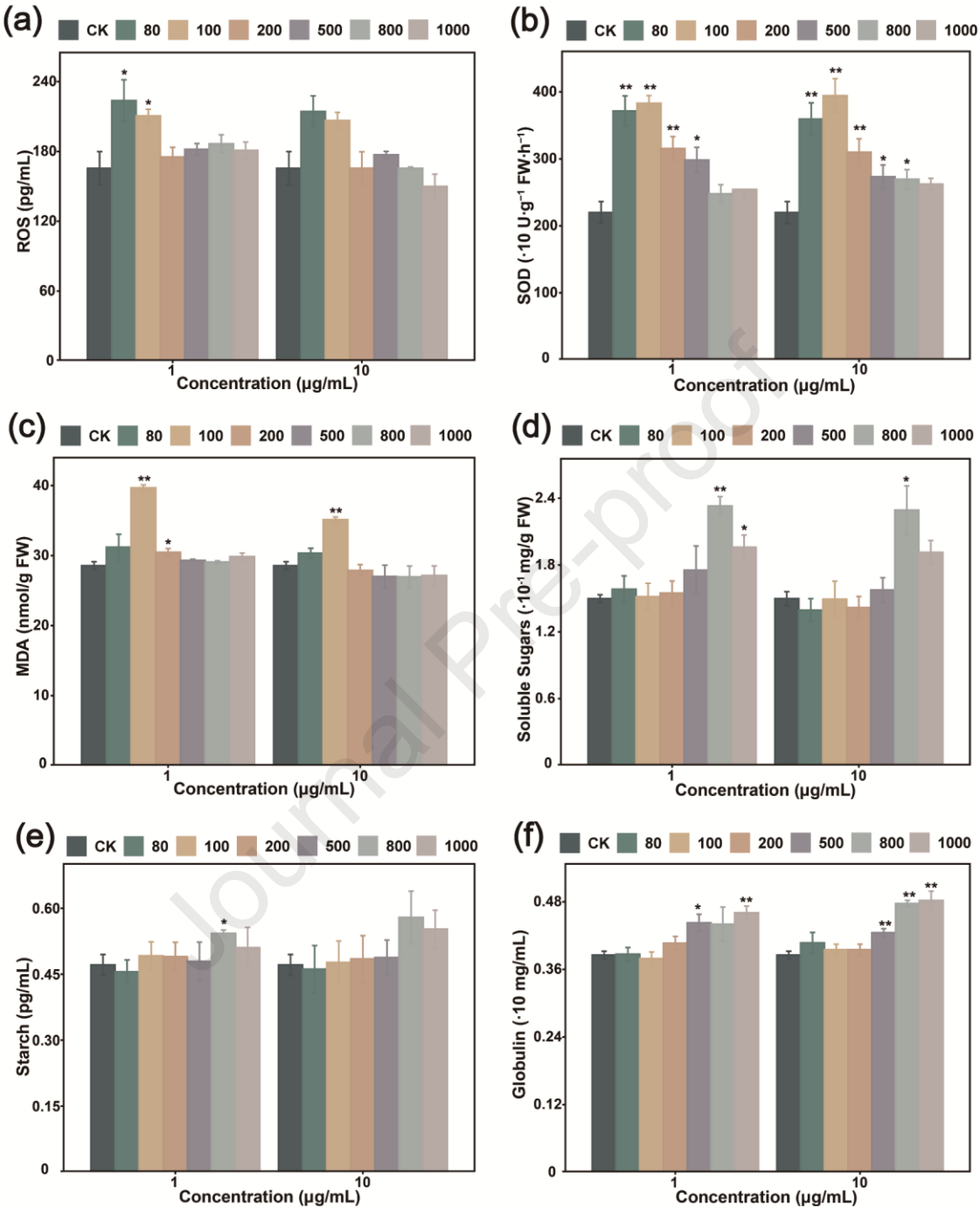

Figure 4. Physicochemical parameters and components of rice leaves after 14 days of exposure to PS MNPs of different particle diameters (80, 100, 200, 500, 800, and 1000 nm) at concentrations of 1 μg/mL and 10 μg/mL, including ROS content (a), SOD enzyme activity (b), MDA content (c), soluble sugars content (d), starch content (e),

globulin content (f). For a given PS MNPs diameter and concentration, significant differences between the control and treatment groups (intergroup comparsion) are marked with * ($P < 0.05$) and ** ($P < 0.01$).

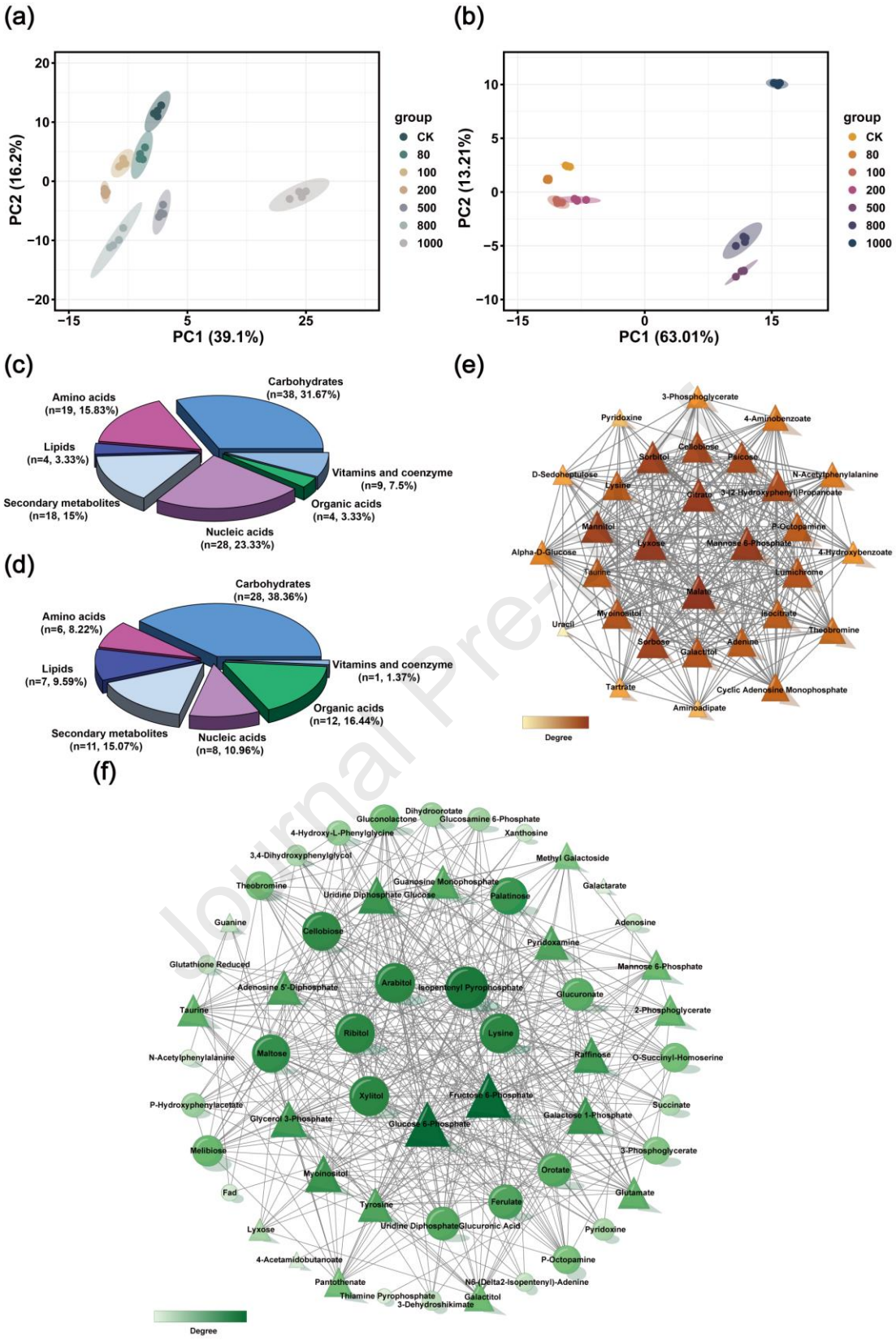

Figure 5. Metabolic anaylsis in rice after 14 days of exposure to PS of different particle diameters (80, 100, 200, 500, 800, and 1000 nm) at concentrations of 1 μg/mL,

including PCA analysis of metabolic differences between PS-exposed and control groups in leaves (a), and roots (b), categorization of differentially expressed metabolites in rice leaves (c) and (d) roots, and metabolites in leaves (f) and roots (e) associated with PS exposure size were identified using weighted gene co-expression network analysis (WGCNA). Darker colors and larger nodes indicate stronger interaction degree; circles represent positive correlations, and triangles represent negative correlations with PS MNPs exposure diameter. The closer to the center of the circle, the higher the degree of interaction with other metabolites.

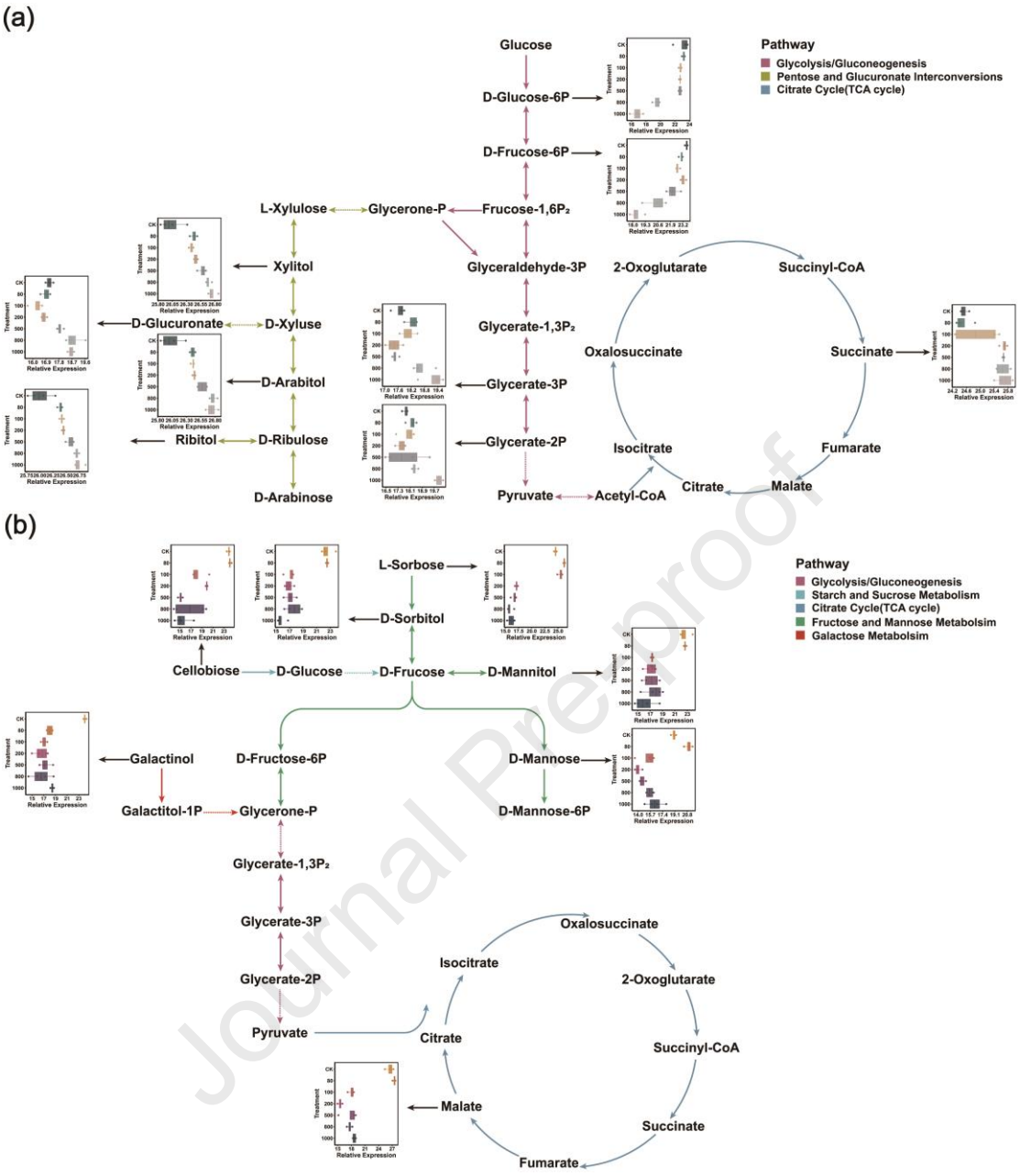

Figure 6. Metabolic network diagrams of rice leaves (a) and roots (b) based on metabolites highly correlated with PS MNPs exposure particle diameters after 14 days, identified via weighted gene co-expression network analysis (WGCNA). Solid and dashed lines represent direct and indirect connections between metabolites, respectively, and arrows indicate the direction of conversion.

Abstract Graphics

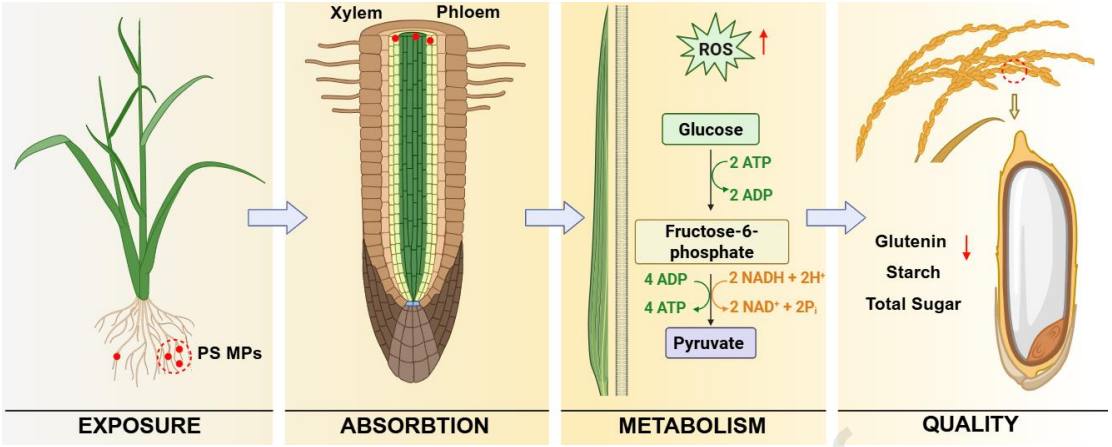

(Created with bioRender.com)

Highlights:

PS MPs size ≤ 100 nm induce ROS accumulation in rice and lead to reduced glutenin content in the grains.

The glycolysis/gluconeogenesis, as well as pentose and glucuronate interconversion pathway, is strongly associated with the particle size of PS MPs exposure.

Rice upregulates carbohydrate metabolism, promoting sugar accumulation to counter PS MPs stress.

Declaration of interests

☒ The authors declare that they have no known competing financial interests or personal relationships that could have appeared to influence the work reported in this paper.

☐ The authors declare the following financial interests/personal relationships which may be considered as potential competing interests: